# Structural Homology Discloses a Bifunctional Structural Motif at the N-Termini of $G_\alpha$ Proteins†

Mickey Kosloff,‡ Natalie Elia,‡ and Zvi Selinger*

*Department of Biological Chemistry and Kühne Minerva Center for Studies of Visual Transduction, Institute of Life Sciences, The Hebrew University, Givat Ram, Jerusalem 91904, Israel*

*Received August 26, 2002; Revised Manuscript Received October 7, 2002*

ABSTRACT: In a family of proteins, often the three-dimensional structure has been experimentally determined only for one member or a few members of the family. Homology modeling can be used to model the structures of all other members of the family and thus allow comparison of these structures. This approach was applied to heterotrimeric G proteins that require anchorage to the plasma membrane to properly interact with membrane-bound receptors and downstream effectors. Lipid modification by palmitoylation is a fundamental contributor to this localization, but the signals leading to this modification are still unknown. In this work, homology models of all the different human $G_\alpha$ paralogs were generated using automated homology modeling, and the electrostatic potential of these proteins was calculated and visualized. This approach identifies a basic, positively charged, structural motif in the N-termini of heterotrimeric G proteins, which is not readily discernible from sequence alone. The basic motif is much reduced in those $G_\alpha$ subunits that also undergo myristoylation, suggesting that the basic patches and myristoylation play overlapping roles. These motifs can affect both membrane affinity and orientation and determine the palmitoylation of $G_\alpha$ subunits in cooperation with the $G_{\beta\gamma}$ subunits, as has been corroborated by previous experimental studies. Furthermore, other palmitoylated proteins such as GAP-43 and RGS proteins share this α-helical basic motif in their N-terminus. It therefore appears that this structural motif is more widely applicable as a membrane-targeting and palmitoylation-determining signal. The work presented here highlights the possibilities available for experimentalists to discover structural motifs that are not readily observed by analysis of the linear sequence.

Heterotrimeric ($\alpha\beta\gamma$) G proteins relay signals between cell surface receptors and membrane-bound effectors in numerous signaling cascades. To ensure specificity, effective concentrations, and speed of interactions, these signaling components are usually localized to the membrane domain. The $G_\alpha$ proteins are anchored to the membrane by one or more lipid modifications at their N-termini. These modifications are the reversible, post-translational palmitoylation (also known as S-acylation), the stable, cotranslational myristoylation, or both (reviewed in refs *1*−*5*). While the consensus sequence for myristoylation has been well characterized (*6*), no sequence determinant for palmitoylation has been identified (*2*, *5*).

The localization of α subunits to the plasma membrane has been explained by the "two-signal model" (reviewed in refs *3* and *4*). This model suggests that peripheral membrane proteins such as $G_\alpha$ subunits require more than one signal to firmly attach them to the plasma membrane. Palmitoylation provides such a strong anchor, but the currently held view is that a protein must first be targeted to the plasma membrane to undergo this modification (*4*, *5*, *7*).

In the case of $G_\alpha$ subunits that undergo myristoylation (Gi, Go, etc.), two such complementing membrane-targeting signals were shown to be myristoylation and interaction with the $\beta\gamma$ subunit complex, which carries a hydrophobic prenyl moiety on the $\gamma$ subunit (*3*−*5*). For $G_\alpha$ subunits that undergo only palmitoylation (Gs, Gq, etc.), the single known relevant targeting signal is their affinity for the $\beta\gamma$ subunits (*3*, *8*, *9*). Recent reports, however, suggested the possible existence of an additional, unidentified signal that determines membrane localization for this subfamily (*3*, *10*−*13*).

To visualize putative membrane-targeting signals in a three-dimensional context, we constructed homology models of all different human $G_\alpha$ paralogs. We found that all α subunits modified only by palmitoylation contain a similar structural motif at their N-terminus. This structure is characterized by a prominent, positively charged patch on one side of the α-helical N-terminus of the α subunits and is more prominent in $G_\alpha$ proteins that do not undergo myristoylation. This structural motif is oriented opposite to the face that interacts with the $\beta\gamma$ subunits. Therefore, the positive patches are free to interact with the negatively charged inner surface of the plasma membrane in both the monomeric and trimeric forms of the α subunit. Most likely, this electrostatic interaction will enhance the affinity of these $G_\alpha$ subunits for the plasma membrane and affect their orientation. The N-terminus of a $G_\alpha$ protein can therefore be described as amphiphilic, containing dual signals attracting

† This work was supported by grants from the NIH (EY-03529), the Moscona Foundation, and the Minerva Foundation.

* To whom correspondence should be addressed: Department of Biological Chemistry, Institute of Life Sciences, The Hebrew University, Givat Ram, Jerusalem 91904, Israel. Telephone: +972-2-6585419. Fax: +972-2-6527427. E-mail: selinger@vms.huji.ac.il.

‡ These authors contributed equally to this work.

10.1021/bi026729x CCC: $22.00 
Published on Web 11/14/2002

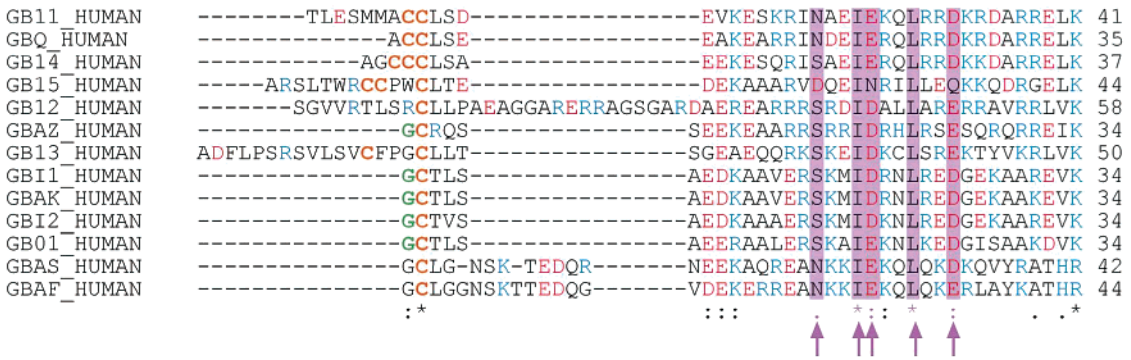


FIGURE 1: No sequence motif for palmitoylation is apparent in the $G_\alpha$ subunits that undergo palmitoylation. The alignment is of residues from the N′ to the first conserved residue of the GTPase domain and was done using ClustalW (EBI). Many of the conserved residues directly interact with the $\beta\gamma$ complex (marked in purple). The cysteines that are available for palmitoylation are marked in orange, glycines that undergo myristoylation in green, basic residues in blue, and acidic residues in red. The sequences are annotated by their Swissprot ID and correspond (by order of appearance) to the N-terminal sequences of human $G_{11}$, $G_q$, $G_{14}$, $G_{15}$, $G_{12}$, $G_z$, $G_{13}$, $G_{i1}$, $G_{i3}$, $G_{i2}$, $G_{o1}$, $G_s$, and $G_{olf}$.

it to the membrane in cooperation with the $\beta\gamma$ subunits, thereby enabling it to undergo palmitoylation. As palmitoylation has been shown to modify a plethora of proteins extending beyond G proteins, the presence of such a motif could be widespread among these proteins.

## EXPERIMENTAL PROCEDURES

*Multiple-Sequence Alignments.* The multiple-sequence alignments were done using ClustalW (EBI). The sequences were truncated at the first conserved sequences that belong to the G domain (*14*). Minor corrections were made to improve the alignment of the N-terminal cysteines.

*Helical Wheel Representation.* Helical wheel representations of the N-terminal sequence predicted to be an α helix by the Psi-Pred server (*15*) were mapped to a helical wheel representation using SeqWeb (Accelrys).

*Three-Dimensional Models of $G_\alpha$ Subunits.* Three-dimensional homology models of all human $G_\alpha$ subunits were generated using the Swiss-Model server (*16*). This server automatically searched for homologous protein structures with which to build the model. For the highly conserved globular domain of the protein (the G domain and the helical domain) (*14*), the Swiss-Model server chose as templates most of the many available crystal structures of $G_\alpha$ subunits. For the N-terminal domain, the server used as templates three structures that contain this domain: 1GP2, 1GOT (heterotrimer structures) (*17*, *18*), and 1AGR (Gi-RGS4 structure) (*19*). In all cases, the templates used by the Swiss-Model server were structures of $G_\alpha$ subunits. The secondary structure of the models (especially that of the N-terminus) was confirmed using the Psi-Pred algorithm (*15*) and also by comparison to available crystal structures. Some of the resulting models contain the extreme N-terminus of the protein in one-letter amino acid code, because the templates used to build a homology model do not contain this region.

*Electrostatic Surface Map of $G_\alpha$ Subunits.* The electrostatic potential distribution was calculated using Delphi (*20*) from the InsightII software package (Accelrys). The CFF force field (Accelrys) was employed using van der Waals (VDW) radii, and a full Coulombic calculation was performed using at least a 10 Å boundary extending beyond the longest axis of the protein. The internal protein dielectric constant was 2.0, the water solvent dielectric constant 80.0, its radius 1.4 Å, and the ionic strength 0.145 M (physiological). An energy convergence criterion of $1 \times 10^{-6}$ kcal/mol was applied. Visualization of the results was carried out in InsightII (Accelrys) by mapping the electrostatic potential on the Connolly surface of the protein and by calculating the electrostatic potential surfaces at 1 and −1 kT/e and displaying these as equi-potential contour meshes.

## RESULTS

*There Is No Consensus Sequence for Palmitoylation of $G_\alpha$ Subunits.* A multiple-sequence alignment of the full sequences of G protein α subunits results in an alignment affected by the highly conserved domains common to all members of this family (the G domain and the helical domain; see ref *14* for details). We therefore aligned only the N-terminal sequences of all human $G_\alpha$ paralogs that are less than 90% identical and undergo palmitoylation (Figure 1). Comparison of the residues flanking the cysteins that undergo palmitoylation (marked in orange) does not reveal a sequence motif that might direct palmitoylation, as many of the conserved amino acids are known to interact with the $\beta\gamma$ subunits (marked in purple). Therefore, in agreement with previous reports (*2*, *5*), we did not find a clear consensus sequence determining palmitoylation.

*Positively Charged Patches in the N-Terminus of $G_\alpha$ Subunits.* Previously, the N-termini of $G_\alpha$ subunits were shown to have important roles in determining their localization and interaction with the $\beta\gamma$ subunits (*3*, *9*, *14*, *21*, *22*). Moreover, electrostatics and specifically positive charges in a protein are known to significantly increase its affinity for the negatively charged inner face of the plasma membrane (*4*, *23*−*25*). It is therefore noteworthy that in the N-termini of the human $G_\alpha$ subunits that are modified only by palmitoylation, between 9 and 17 amino acids contain basic, positively charged residues. Since secondary structure prediction and analysis of the available crystal structures (*14*, *22*) suggest an α-helical conformation of this domain, we plotted the sequences of the N′ domain of this $G_\alpha$ family onto helical wheel projections (see Figure 2 for an example). This analysis showed that in all of these cases, nearly all of the positive residues map specifically to one face of the α helix.

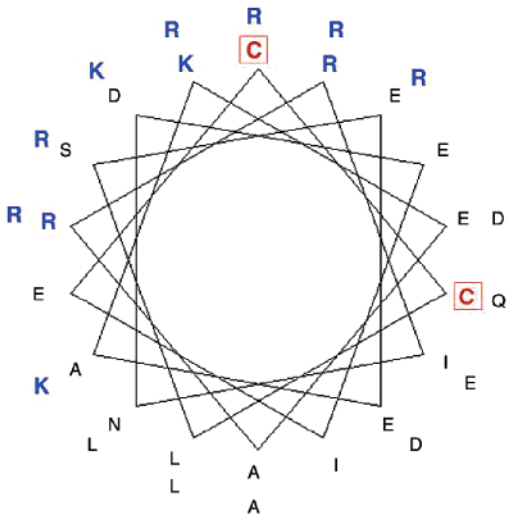


FIGURE 2: Basic residues (marked in blue) map to one face of the N-terminal α helix of $Gq_\alpha$. Residues 3−35 of human $Gq_\alpha$ (see the sequence in Figure 1) were mapped onto a helical wheel representation according to their α-helical secondary structure prediction.

To visualize this motif in a structural context, we used the Swiss-Model server (*16*) to construct homology models of all $G_\alpha$ subunits that are modified only by palmitoylation and are less than 90% identical in their N-termini. We calculated the electrostatic potential for each model (see Experimental Procedures) and mapped it onto its molecular surface (Figure 3a). The secondary structure was verified by comparison to available crystal structures and by secondary structure prediction using the Psi-Pred server (*15*). Comparison of these monomeric models to the available structures of the heterotrimer (*14*, *17*, *18*, *22*) shows that their overall tertiary structure is the same (data not shown). Our models are therefore representative of the monomeric forms of the α subunits that can join with the $\beta\gamma$ subunits and interact with the plasma membrane (*22*).

All of these models exhibit prominent positively charged patches (marked with blue arrows) in their mostly α-helical N-termini (Figure 3a). These basic patches extend a positive potential well beyond the molecular surface of the protein. Because some of the models do not extend all the way to the N-terminus, the actual basic motif might be even larger in these $G_\alpha$ proteins. Furthermore, comparison to the crystal structures of the heterotrimers (*14*, *17*, *18*) shows that these patches are opposite the face of $G_\alpha$ that interacts with the $\beta\gamma$ subunits (Figure 3b). Hence, the positive patches are free to interact with the negatively charged inner face of the plasma membrane, regardless of whether the $G_\alpha$ subunits are in the monomeric or trimeric form. This interaction can therefore serve as a targeting signal to the plasma membrane. As the dual signals of the basic motif and $\beta\gamma$ binding can both confer affinity to the plasma membrane, the N-terminus of these $G_\alpha$ subunits can be best described as amphiphilic. Reciprocally, such interactions with the membrane and the $\beta\gamma$ subunits are expected in turn to stabilize the α-helical secondary structure of the N-terminus and thereby affect its interaction with its signaling partners.

In contrast to the results described in detail above, the positively charged motif is greatly reduced in those $G_\alpha$ subunits that do undergo myristoylation (Figure 3c). Not only is the extent of the basic patches in these $G_\alpha$ subunits much smaller, but negative patches close to the N-terminus are also evident. The latter are expected to reduce even further any membrane affinity that might be due to the basic, positively charged patches. A logical hypothesis arising from these results is that the positively charged motif and the lipid anchor of myristoylation have overlapping roles within the context of the two-signal model. Either motif might be sufficient to act together with the $\beta\gamma$ subunits in targeting $G_\alpha$ subunits to the plasma membrane and to orient them correctly to the palmitoyl transferase enzyme and other signaling proteins.

At first glance, Gz seems to be an exception within the subfamily of $G_\alpha$ subunits that undergo myristoylation, as it has a prominent positive patch. However, this difference correlates to a different biological behavior. In vivo, Gz can undergo phosphorylation on two residues in the midst of the N-terminal basic motif: Ser 17 and Ser 27 (*5*, *26*). The negative charges thus introduced in the N-terminal helix of Gz significantly reduce the extent of the positive patches seen in Figure 3c and probably affect its secondary structure. Phosphorylation could therefore decrease the affinity of Gz for the membrane and change its orientation to the plasma membrane as has indeed been shown for other signaling proteins (*23*, *24*, *27*). This prediction is supported by experiments showing that phosphorylation of Gz inhibits its interaction with specific RGS proteins and with the $\beta\gamma$ subunits (*26*).

*Application to Additional Proteins.* In addition to $G_\alpha$ subunits, numerous other proteins undergo palmitoylation at their N-terminus as the only lipid modification (*4*). Notable examples are neuromodulin/GAP-43, members of the RGS family, the $\beta$ subunit of the voltage-dependent calcium channel, etc. It is therefore highly desirable to determine whether the structural motif described above is more widely applicable as a palmitoylation signal to such targets outside the heterotrimeric G protein family. Unfortunately, there are currently no available crystal structures that contain the relevant domains for GAP-43, RGS proteins, etc. Furthermore, three-dimensional models of these proteins could not be generated by using homology modeling or by the fold recognition server BioInBGU (*28*) because applicable templates could not be found using either of these methods.

Experimental evidence, however, did find basic α-helical motifs at the N-termini of these proteins that conferred affinity for the plasma membrane. Hayashi et al. (*27*) studied the GAP-43 protein using circular dichroism and two-dimensional NMR and reported the existence of an amphiphilic α helix in the N-terminus of this protein. This basic motif was sufficient to target GAP-43 to the plasma membrane. Strikingly, while the conformation of this domain in solution is flexible, binding to the membrane stabilizes an α-helical conformation. Additionally, phosphorylation on a serine residue located in this domain inhibited both the helical conformation and membrane binding. Comparable results were also reported for RGS proteins. The N-terminal domains of RGS4 and RGS16 were shown to be α-helical and to bind negatively charged lipids by a positively charged basic domain (*29*−*31*). Consistently, mutation of the basic residues in these domains to neutral or negatively charged residues disrupted their membrane binding.

To visualize these domains, we constructed an α-helical model of two representative examples: RGS16 (residues 12−29) (*29*) and GAP43 (residues 30−54) (*27*). Both of these

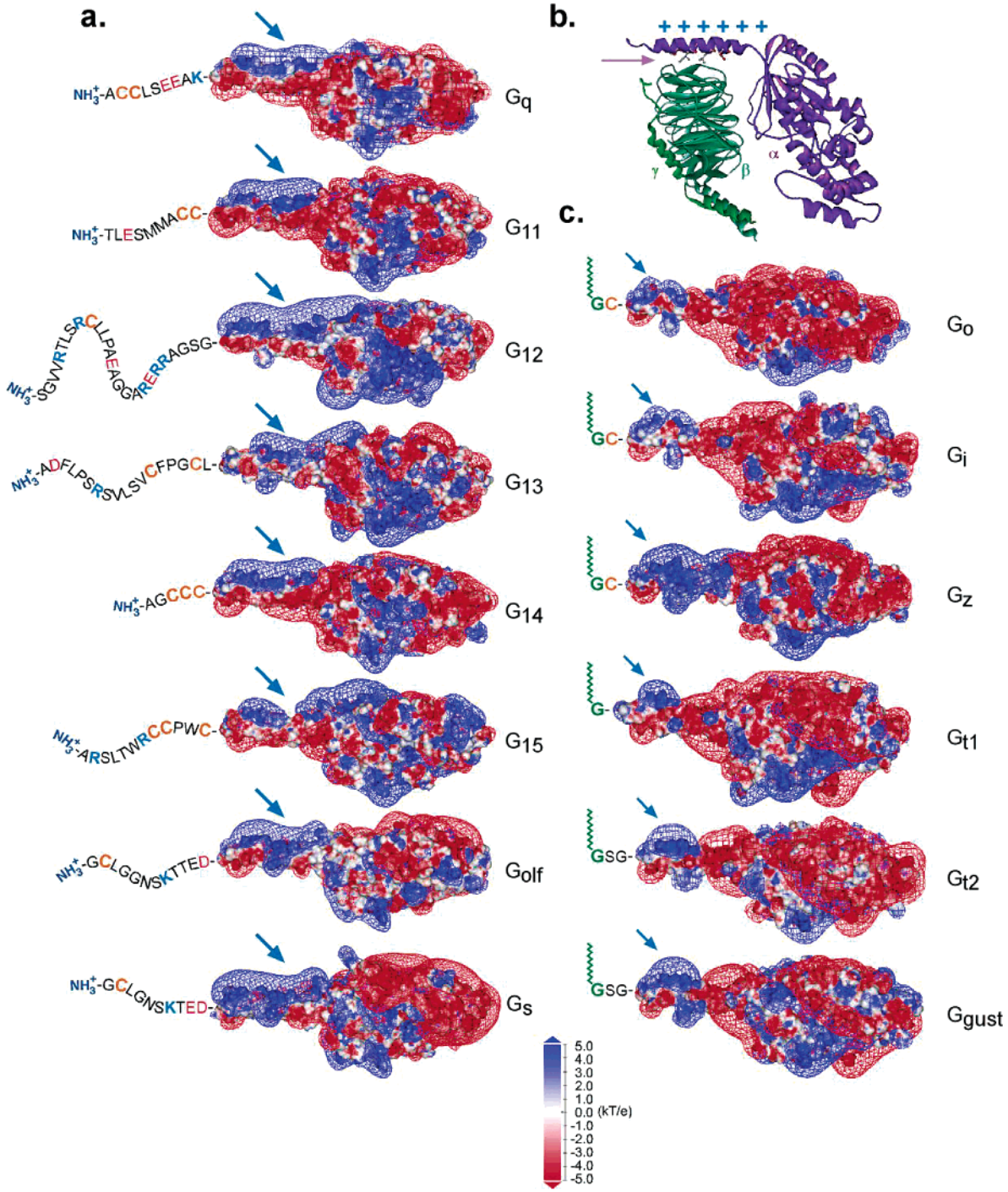


FIGURE 3: Positive patches in the N-termini of $G_\alpha$ subunits. (a) Three-dimensional models of all human $G_\alpha$ subunits that undergo only palmitoylation. Prominent positive patches are evident, extending a positive potential reaching significantly beyond the molecular surface of the protein (marked with blue arrows). (b) Comparison to the crystal structures of the heterotrimer shows that the face of the N-terminal α helix that binds the $\beta\gamma$ subunits is on the opposite side of the positive patch. The structure of the Gi heterotrimer (adapted from ref *17*) is shown as a ribbon representation, with the conserved residues interacting with the $\beta\gamma$ subunits shown in ball-and-stick representation (marked with purple arrow). The orientation of the positive patches in the relevant $G_\alpha$ subunits (in panel a) is depicted with plus symbols. (c) Three-dimensional models of all human $G_\alpha$ subunits that undergo myristoylation. In comparison to panel a, the positive patches are much smaller and substantial negative patches are evident nearby. The electrostatic color coding (bottom of figure) corresponds to panels a and c. The electrostatic potential calculated by Delphi was mapping onto the Connolly molecular surface of the models. Superimposed over the molecular surfaces are the electrostatic equipotential contours at 1 (blue mesh) and −1 kT/e (red mesh).

models exhibited a marked positive potential extending well beyond the molecular surface of the peptides (Figure 4). The similarity between these peptides and the structural motif we identified in $G_\alpha$ subunits suggests that this motif might represent a widespread signal for membrane targeting and subsequent palmitoylation.

## DISCUSSION

In this work, we investigated the N-terminal domain of all the different human $G_\alpha$ paralogs. Characterization of the enzymes that underlie the palmitoylation-depalmitoylation cycle of $G_\alpha$ subunits and its regulation has been unfortunately

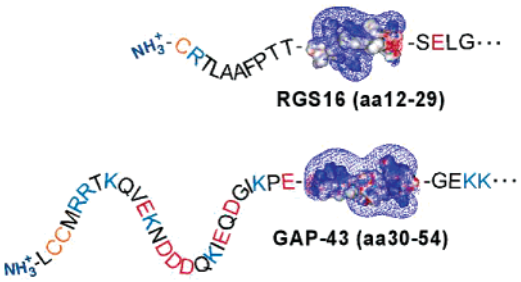


FIGURE 4: Positive patches in the N-terminus of GAP-43 and RGS16. The models are of residues 12−29 of RGS16 and of residues 30−54 of GAP43. The electrostatic potential calculated by Delphi was mapped onto the Connolly molecular surface of the models. Superimposed over the molecular surfaces are the electrostatic equipotential contours at 1 (blue mesh) and −1 kT/e (red mesh).

hindered because of technical difficulties (*3*−*5*). Therefore, a careful examination of the substrates for palmitoylation can shed more light on these processes. Consistent with previous reports, we did not find a clear sequence motif for palmitoylation in the N-terminus of $G_\alpha$ subunits. On the structural level, however, we found an electrostatically positive basic motif that is shared by $G_\alpha$ subunits that are modified only by palmitoylation. In contrast, the magnitude of this positive patch is much smaller in α subunits that also undergo myristoylation. Since it has been suggested that the palmitoylation of $G_\alpha$ proteins is determined by prior targeting to the plasma membrane, this positive motif can confer affinity for the negatively charged inner face of the membrane, as well as for recognition by the palmitoyl transferase enzyme. We suggest that the structural motif we identified and myristoylation have overlapping roles in assisting a $G_\alpha$ subunit to reach the plasma membrane and undergo palmitoylation (Figure 5). Since the N-terminal α helix that contains the positive motif also interacts with the $\beta\gamma$ complex, it can be defined as amphiphilic, containing dual attractive motifs. One signal for this membrane localization might therefore be *either* myristoylation or the novel motif that we identified. The second signal targeting $G_\alpha$ subunits to the plasma membrane is their affinity for the $\beta\gamma$ complex. Such two signals can be expected to work synergistically in conferring affinity of $G_\alpha$ subunits for the membrane and thereby play an instrumental role in their subsequent palmitoylation. The cooperativity of two signals (myristoylation and a basic motif) has indeed been extensively characterized for the Src protein (*23*, *24*).

Numerous experimental results support our revised model for the two-signal model for the membrane attachment of $G_\alpha$ subunits. The positive motif we identified might account, at least partly, for the additional membrane-targeting signal suggested in refs *10*, *12*, and *13*. Jones and Gutkind recently suggested that the positive residues in the N-terminus of $G_{12}$ might contribute to the membrane targeting observed for acylation mutants of $G_{12}$ (*11*). A recent study showed a

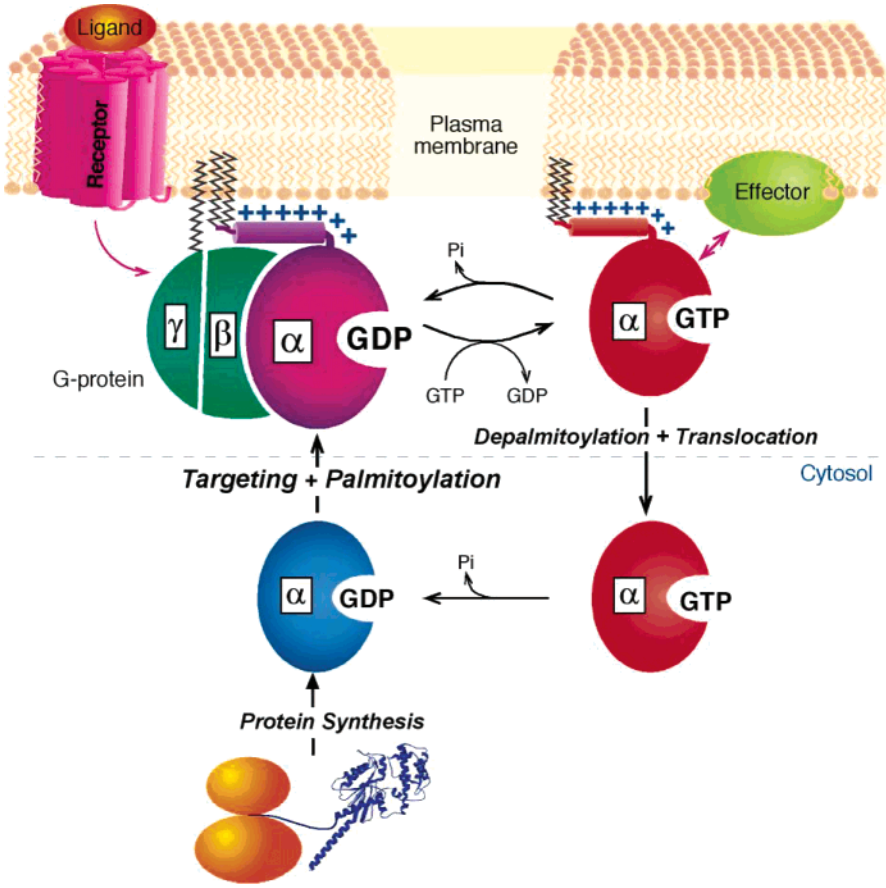


FIGURE 5: Putative model for the targeting of $G_\alpha$ subunits to the plasma membrane. The newly synthesized $G_\alpha$ subunits, or alternatively, $G_\alpha$ subunits that have translocated to the cytosol, are targeted to the membrane by two cooperative signals. These are the $\beta\gamma$ complex and the basic motif in the N-terminal α helix. The resulting transient membrane attachment is followed by palmitoylation that firmly attaches the $G_\alpha$ subunits to the plasma membrane. While the figure depicts a doubly palmitoylated $G_\alpha$ (such as Gq), other $G_\alpha$ subunits can undergo a similar cycle with one site of palmitoylation. In $G_\alpha$ subunits that undergo myristoylation (not shown), it partly replaced the basic motif.

connection between positive residues of $Gq_\alpha$ and $Gs_\alpha$ and the $\beta\gamma$ subunits (*9*). In this work, one of the basic residues that points away from the $\beta\gamma$ interacting face and belongs to the positive motif mentioned above was mutated to an alanine. This mutation somewhat reduced the affinity of these proteins for the $\beta\gamma$ subunits and also diminished their degree of membrane attachment. Additional mutations in residues that interact with the $\beta\gamma$ subunits synergistically decreased the extent of these interactions and also reduced the level of palmitoylation of these $G_\alpha$ subunits. In the case of the G protein Gi, it was shown that excess $\beta\gamma$ subunits rescued the extent of both the membrane localization and palmitoylation of a nonmyristoylated, α subunit mutant (*7*).

It is interesting to note that structural studies of $G_\alpha$ subunits have shown that their N-terminus can change its conformation due to different activation states (eloquently reviewed in ref *14*). This fact suggests the possibility that the interaction of these $G_\alpha$ subunits with their environment, as mediated by their N-terminal domain, can be allosterically regulated by different proteins. Putatively, dissociation of the heterotrimer or interaction with proteins other than the $\beta\gamma$ subunits might result in a conformation of $G_\alpha$ different from that seen in our models. Such an allosteric change will inhibit its interactions both with $\beta\gamma$ subunits and with the membrane and might also enable efficient translocation of $G_\alpha$ to the cytosol, depending on prior depalmitoylation (*2*, *3*, *5*). The connection between conformation and localization has been shown for other membrane-binding motifs and is emerging as a theme for amphitropic proteins, proteins that can cycle between the membrane and the cytosol (*32*). The importance of the correct conformation of the N-terminus of $G_\alpha$ subunits was indeed shown experimentally when chimeras of this domain of $Gq_\alpha$ and $Gs_\alpha$ fused to GFP failed to target the membrane and remained soluble (*9*).

It should be pointed out that this basic motif can play additional roles. It can direct $G_\alpha$ proteins to a specific, favorable orientation toward the plasma membrane and relative to other proteins with which it interacts. Notable examples are the specific thioesterase and protein-palmitoyl transferase that detach and reattach the palmitates to the $G_\alpha$ protein. With the absence of a clear sequence consensus for palmitoylation, the basic structural motif might be instrumental in the specific recognition of the relevant substrates by the protein-palmitoyl transferase.

Our work shows the existence of structural motifs that are not readily observed by analysis of the linear sequence and lays the basis for applying this methodology to other, newly discovered proteins. Furthermore, as is evident from experimental studies and our structural analysis, other palmitoylated proteins such as GAP-43 and RGS proteins share this α-helical basic motif in their N-termini. It appears therefore that this structural motif might be added to the list of membrane-targeting motifs that includes C1, C2, PH domains, and others.

## ACKNOWLEDGMENT

We thank Deborah Shalev for technical assistance and Hanah Margalit, Daniel Fischer, and Roger Kornberg for helpful discussion.

## REFERENCES

1. Milligan, G., Grassie, M. A., Wise, A., MacEwan, D. J., Magee, A. I., and Parenti, M. (1995) *Biochem. Soc. Trans. 23*, 583−587.
2. Mumby, S. M. (1997) *Curr. Opin. Cell Biol. 9*, 148−154.
3. Wedegaertner, P. B. (1998) *Biol. Signals Recept. 7*, 125−135.
4. Resh, M. D. (1999) *Biochim. Biophys. Acta 1451*, 1−16.
5. Chen, C. A., and Manning, D. R. (2001) *Oncogene 20*, 1643−1652.
6. Maurer-Stroh, S., Eisenhaber, B., and Eisenhaber, F. (2002) *J. Mol. Biol. 317*, 523−540.
7. Degtyarev, M. Y., Spiegel, A. M., and Jones, T. L. (1994) *J. Biol. Chem. 269*, 30898−30903.
8. Iiri, T., Backlund, P. S., Jr., Jones, T. L., Wedegaertner, P. B., and Bourne, H. R. (1996) *Proc. Natl. Acad. Sci. U.S.A. 93*, 14592−14597.
9. Evanko, D. S., Thiyagarajan, M. M., and Wedegaertner, P. B. (2000) *J. Biol. Chem. 275*, 1327−1336.
10. Ammer, H., and Schulz, R. (1997) *Mol. Pharmacol. 52*, 993−999.
11. Jones, T. L., and Gutkind, J. S. (1998) *Biochemistry 37*, 3196−3202.
12. Huang, C., Duncan, J. A., Gilman, A. G., and Mumby, S. M. (1999) *Proc. Natl. Acad. Sci. U.S.A. 96*, 412−417.
13. Hughes, T. E., Zhang, H., Logothetis, D. E., and Berlot, C. H. (2001) *J. Biol. Chem. 276*, 4227−4235.
14. Sprang, S. R. (1997) *Annu. Rev. Biochem. 66*, 639−678.
15. Jones, D. T. (1999) *J. Mol. Biol. 292*, 195−202.
16. Peitsch, M. C. (1996) *Biochem. Soc. Trans. 24*, 274−279.
17. Wall, M. A., Coleman, D. E., Lee, E., Iniguez-Lluhi, J. A., Posner, B. A., Gilman, A. G., and Sprang, S. R. (1995) *Cell 83*, 1047−1058.
18. Lambright, D. G., Sondek, J., Bohm, A., Skiba, N. P., Hamm, H. E., and Sigler, P. B. (1996) *Nature 379*, 311−319.
19. Tesmer, J. J. G., Berman, D. M., Gilman, A. G., and Sprang, S. R. (1997) *Cell 89*, 251−261.
20. Nicholls, A., and Honig, B. (1991) *J. Comput. Chem. 12*, 435−445.
21. Hepler, J. R., Biddlecome, G. H., Kleuss, C., Camp, L. A., Hofmann, S. L., Ross, E. M., and Gilman, A. G. (1996) *J. Biol. Chem. 271*, 496−504.
22. Bohm, A., Gaudet, R., and Sigler, P. B. (1997) *Curr. Opin. Biotechnol. 8*, 480−487.
23. Murray, D., Ben-Tal, N., Honig, B., and McLaughlin, S. (1997) *Structure 5*, 985−989.
24. Murray, D., Hermida-Matsumoto, L., Buser, C. A., Tsang, J., Sigal, C. T., Ben-Tal, N., Honig, B., Resh, M. D., and McLaughlin, S. (1998) *Biochemistry 37*, 2145−2159.
25. Murray, D., McLaughlin, S., and Honig, B. (2001) *J. Biol. Chem. 276*, 45153−45159.
26. Ho, M. K., and Wong, Y. H. (1998) *Biol. Signals Recept. 7*, 80−89.
27. Hayashi, N., Matsubara, M., Titani, K., and Taniguchi, H. (1997) *J. Biol. Chem. 272*, 7639−7645.
28. Fischer, D. (2000) *Pac. Symp. Biocomput.*, 119−130.
29. Chen, C., Seow, K. T., Guo, K., Yaw, L. P., and Lin, S. C. (1999) *J. Biol. Chem. 274*, 19799−19806.
30. Bernstein, L. S., Grillo, A. A., Loranger, S. S., and Linder, M. E. (2000) *J. Biol. Chem. 275*, 18520−18526.
31. Tu, Y., Woodson, J., and Ross, E. M. (2001) *J. Biol. Chem. 276*, 20160−20166.
32. Johnson, J. E., and Cornell, R. B. (1999) *Mol. Membr. Biol. 16*, 217−235.

BI026729X